

## 车载光电经纬仪支撑平台稳定性研究

高庆嘉,王冲,王强龙,王晓明,余毅,刘震宇,刘岩俊\*

中国科学院长春光学精密机械与物理研究所,吉林 长春 130033

**摘要** 传统的车载支撑平台晃动量较大,难以满足车载光电经纬仪高精度不落地测量要求。为了兼顾轻量化、高刚度和便于制造的要求,采用离散体桁架拓扑优化方法设计了一种具有桁架蒙皮式结构的高比刚度车载支撑平台;建立了平台系统的有限元仿真模型,根据平台安装光电经纬仪的稳定性要求,分析了不同工况和载荷条件下平台系统的静力学和模态特性,搭建了支撑平台稳定性实验装置。结果表明,在经纬仪工作角加速度  $0.5(^{\circ})/s^2 \sim 20(^{\circ})/s^2$  范围的激励下,经纬仪基座的响应加速度为  $0.008 \sim 0.55 \text{ m/s}^2$ ,无明显影响经纬仪跟踪性能的共振响应发生。同时,采用倾角传感器测量了平台晃动幅值,最大晃动量为  $7.2''$ 。该支撑平台具有较高的支撑稳定性,适用于车载光电经纬仪高精度不落地测量。

**关键词** 车载光电经纬仪;不落地测量;支撑平台;稳定性

**中图分类号** TH743 **文献标志码** A

**DOI:** 10.3788/AOS230948

## 1 引言

光电经纬仪利用光学成像采集飞行目标信息,经时空配准、交汇计算等处理可以得到所需的目标参数,是现代靶场的重要光测设备<sup>[1-3]</sup>。近年来,随着实战化训练不断深化拓展,多平台机动布站等更多任务的需求,车载光电经纬仪已成为主要发展趋势<sup>[1,4]</sup>。传统的车载光电经纬仪由全挂或半挂车载运输,到达指定场坪后,落至水平地基环上固定,测量精度较高,但操作复杂,且受场地限制。对于车载光电经纬仪不落地测量方式,经纬仪不依赖于地基环,即到达点位驻车后,在车载平台上开展测量工作,该方式摆脱了传统测量站点的位置约束,具备机动性强、布设和展开快速等特点,能够更好地适应靶场实验任务的发展。

经纬仪工作时,相对车载平台运动,产生位置和姿态的晃动。该晃动量较大,成为制约车载光电经纬仪进行高精度测量的重要因素,需要采取合理的措施加以克服。文献[5]提出以经纬仪载车副车架作为车载平台的设计思路,平台稳定精度达到  $20''$ 。文献[6]分析了车载平台变形对光电经纬仪指向精度的影响,由于平台晃动量为  $\pm 42''$ ,采用非接触式测量方法对其进行测量和修正,经纬仪指向精度达  $20''$ 。文献[7-9]针对车载平台具有  $50'' \sim 300''$  晃动的特点,分别采取了误差补偿法、二维查表法、位姿估计法等进行事后修正,使经纬仪指向精度提高到  $16''$ 。可以看到,由于受到尺寸、重量、承载能力和经纬仪跟踪特性等方面的限制,车载平台往往很难

达到较高的稳定性,晃动量超过了几十角秒,难以满足高精度不落地测量要求。采用合适的修正方法能够提高经纬仪的指向精度,但时效性受到限制。

本文兼顾高刚度、轻量化和便于制造的要求,采用离散体桁架拓扑优化方法,设计了一种具有桁架蒙皮式结构的高比刚度车载支撑平台;采用有限元仿真方法分析了不同工况和载荷条件下平台系统的静力学和动力学特性;完成了平台系统的稳定性实验。在搭载质量为  $3000 \text{ kg}$ 、角加速度为  $0 \sim 20(^{\circ})/s^2$  的经纬仪进行工作时,支撑平台最大晃动量为  $7.2''$ ,车载光电经纬仪实时指向精度优于  $15''$ 。

## 2 工作原理

传统的车载光电经纬仪由全挂或半挂车载运输,到达指定场坪后,落至水平地基环上固定,如图 1 所示,操作较为复杂,且受场地限制。所述的车载支撑平台安装于独立底盘越野载车上,如图 2 所示,车载支撑平台上部安装光电经纬仪,下部与载车副车架可分离式安装。工作时,支撑平台与副车架完全脱离,从物理层面隔绝了人员走动、油机振动等影响;另外,设备迎风面积明显减小,风载影响可忽略。

由于采用车载支撑平台代替传统地基环作为测量基座,支撑平台的稳定性成为车载光电经纬仪实现高精度不落地测量的关键因素。支撑平台静态刚度不足则导致测量基座变形过大,引起经纬仪垂轴误差增大,降低经纬仪的指向精度;支撑平台动态刚度不足,既限

收稿日期: 2023-05-09; 修回日期: 2023-06-08; 录用日期: 2023-06-15; 网络首发日期: 2023-06-25

基金项目: 国家自然科学基金(51675506)

通信作者: \*liuyanjun@ciomp.ac.cn

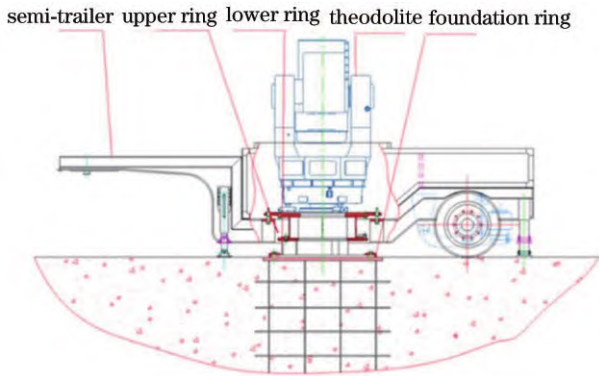


图 1 经纬仪落至地基环工作示意图

Fig. 1 Operation schematic for theodolite landing on foundation ring



图 2 车载支撑平台工作原理图

Fig. 2 Functional diagram of supporting platform

制经纬仪的伺服系统控制带宽,跟踪性能变差,又引起平台晃动,降低经纬仪的指向精度;同时,为保证车载系统的机动性和灵活性,支撑平台要满足轻量化和小型化的要求。

### 3 设计方法

#### 3.1 优化模型

拓扑优化是一种基于目标函数灵敏度信息的设计

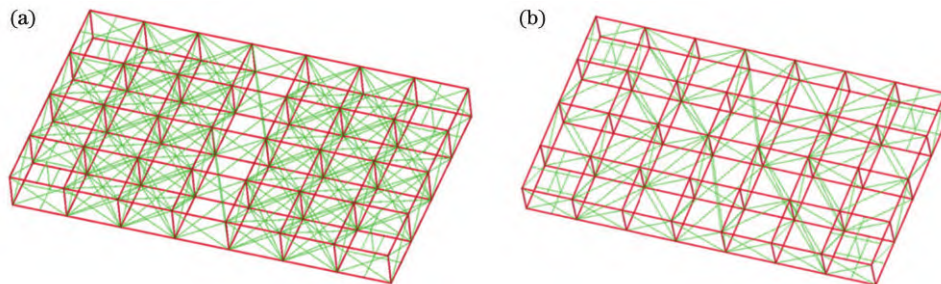


图 3 优化模型中的设计域(细线)与非设计域(粗线)。(a) 原始构型;(b) 优化构型

Fig. 3 Design domain (thin lines) and non-design domain (bold lines) in the optimization model. (a) Original layout; (b) optimal layout

### 4 稳定性仿真分析

#### 4.1 静力学分析

经纬仪的质量、方位和俯仰轴的动态扭矩是影响支撑平台稳定性的重要因素。仿真分析时,以拓扑优化结果为基础,以桁架单元建立支撑平台的有限元模

方法。它根据载荷、边界条件及指定目标(如变形量、柔度等)来确定设计域中材料的分布及其位置,是解决车载支撑平台无法满足高刚度、宽频率和轻量化要求问题的有效方法<sup>[10-12]</sup>。本文采用离散体桁架拓扑优化设计方法对支撑平台进行设计。

工程实际中,设计杆系结构的分布时须综合考虑杆件的抗扭和抗弯特性,仅仅依赖于拉压载荷设计的桁架最优分布仍旧有待于进一步提升。考虑到杆件抗扭和抗弯刚度的近似等效桁架离散设计方法的表达式为

$$\begin{aligned} \min_{\rho_e} \quad & C(\rho_e) = U^T K U \\ \text{s.t.} \quad & K U = F \\ & \sum_{e=1}^{N_E} \rho_e V_e \leq V_{\max} \\ & 0 \leq \rho_{\min} \leq \rho_e \leq 1, \quad e = 1, 2, \dots, N_E, \end{aligned} \quad (1)$$

式中: $C$ 表示结构柔度; $K$ 表示有限元刚度矩阵; $F$ 表示载荷向量; $U$ 表示位移向量; $\rho_e$ 表示单元相对密度; $N_E$ 是总单元个数; $V_e$ 是单元体积; $V_{\max}$ 是要求的体积上限; $\rho_{\min}$ 是单元相对密度的下限。

#### 3.2 优化结果

根据平台外形基本尺寸建立平台框架和支撑结构的有限元网格,确定设计域与非设计域,如图 3(a)所示。针对设计域单元建立拓扑优化设计变量,采用 solid isotropic material with penalization(SIMP)插值方法,以结构柔度的最小化为目标,以体积分数为约束,以经纬仪质量为外载荷,采用 optimality criteria(OC)法进行优化迭代求解,迭代历程如图 4 所示,目标值经过 8 次迭代后得到收敛,相比优化前降低了 70.5%。优化得到的平台构型如图 3(b)所示,除非设计域,设计的杆件整体呈由中间负载区域向平台四角方向扩展的 X 形分布趋势。

型,对集成在平台台面上的光电经纬仪进行简化,保证经纬仪质量、质心和转动惯量不变,以集中质量模型的方式模拟。经纬仪重力为 30000 N,作为静态载荷施加。经纬仪俯仰转动惯量为 120 kg·m<sup>2</sup>,方位转动惯量为 450 kg·m<sup>2</sup>,最大角加速度为 20 (°)/s<sup>2</sup>,作为平台系统动态载荷输入。建立的包括支撑平台、经纬仪和

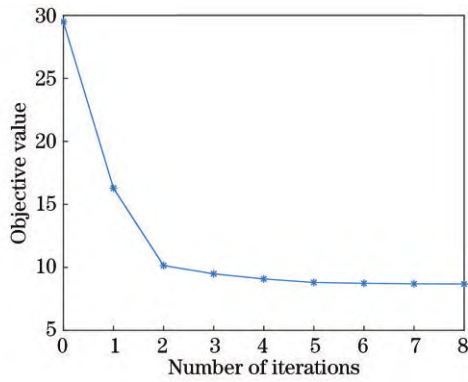


图4 优化迭代历程

Fig. 4 Optimal iterative process

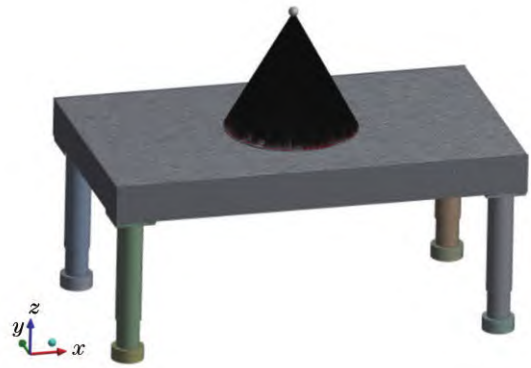


图5 平台系统仿真模型

Fig. 5 Simulation model of the platform system

支腿在内的平台系统的有限元仿真模型如图 5 所示。

图 6 显示了重力载荷作用下平台变形情况,平台最大变形量为 0.142 mm,发生在经纬仪安装面位置。

提取经纬仪安装面上三个方向的位移云图,其中 X 和 Y 向位移变化比较小,可以忽略。Z 方向各节点的变形最大差值为 20.9  $\mu\text{m}$ ,计算得到重力载荷引起的平台在经纬仪安装面的倾斜量为 3.9”。

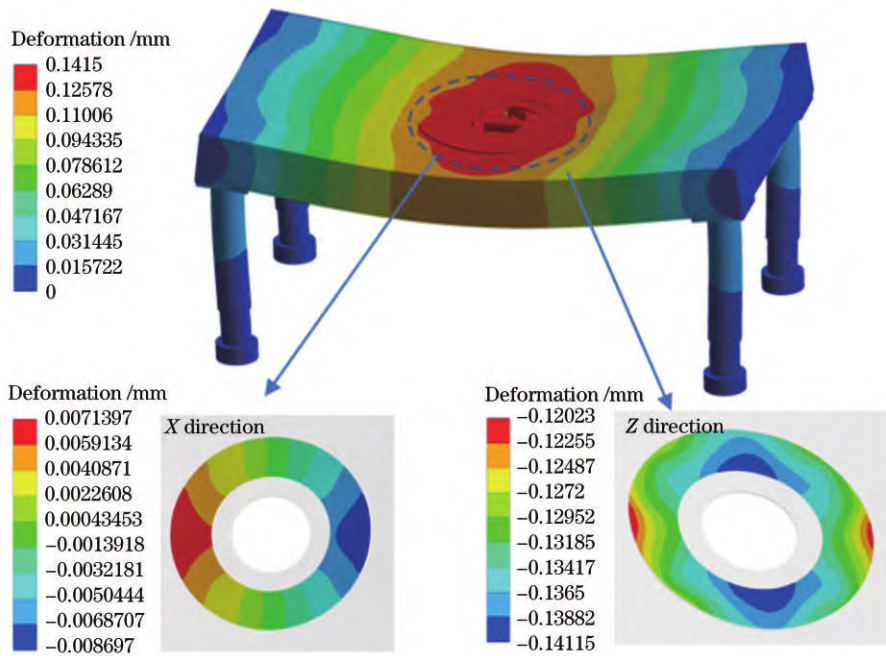


图6 平台受重力载荷影响的位移云图

Fig. 6 Displacement cloud map of the platform affected by gravity load

采用上述仿真方法,得到了平台优化前后的性能对比,如表 1 所示。可以看出,在保证平台刚度基本不变的前提下,相比优化前,优化后的平台质量相对减小了 411.1 kg,有效提高了支撑平台的比刚度。

进一步分析了平台受到经纬仪沿着平台的长度(X向)、宽度(Y向)和高度(Z向)三个方向的动态扭矩综合作用下在经纬仪安装面的变形情况,如图 7 所示。可以看出,在各方向扭矩作用下安装面的变形量大小相近,变形差值最大为 22.6  $\mu\text{m}$ ,引起经纬仪安装面的倾斜量为 4.3”。

表 1 优化前后平台的性能参数对比

Table 1 Comparison of performance parameters of the platform before and after optimization

Parameter	Original platform	Optimized platform	Deviation
Mass of the truss/kg	1551.7	1140.6	-411.1
Max deformation/ $\mu\text{m}$	17.1	20.9	3.8 (0.71”)
First mode frequency/Hz	20.2	19.2	1.0

载的能力。

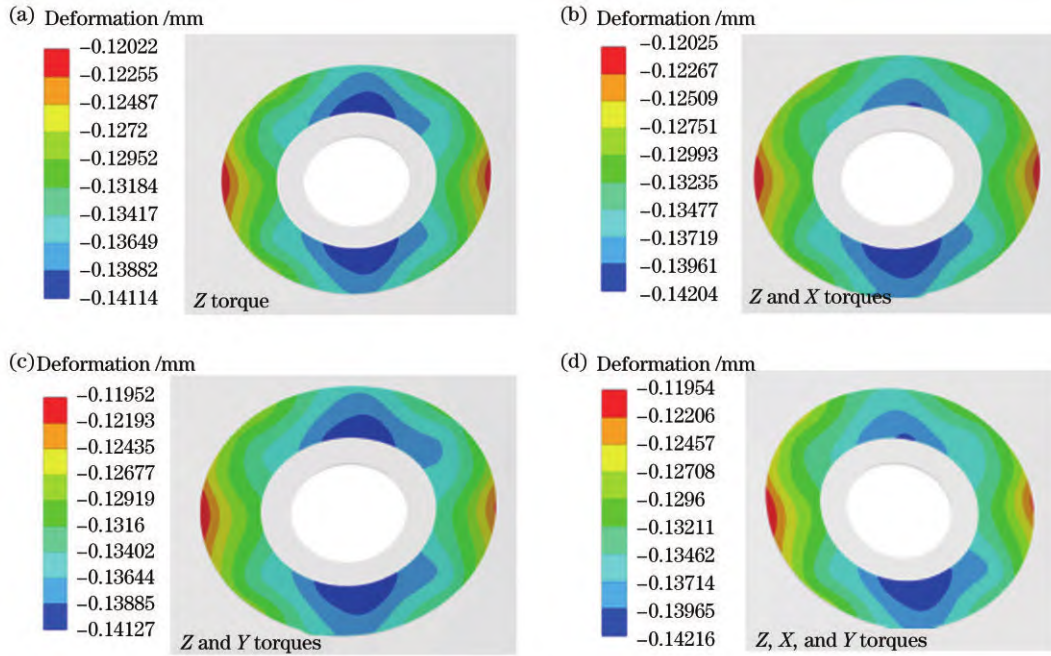


图 7 平台受力矩载荷影响的位移云图

Fig. 7 Displacement cloud maps of the platform affected by torque load

#### 4.2 模态分析

进行模态分析,采用基于预应力的模态分析法提取了平台系统的模态参数,评估其刚度特性。获得的平台前四阶模态频率如表 2 所示,模态振型如图 8 所

示。可以看出:一阶振型是发生在平台宽度方向的弯曲变形;一阶固有频率为 19.2 Hz,平台系统能够为光电经纬仪的不落地测量提供足够的支撑刚度,同时满足控制系统对带宽的指标要求。

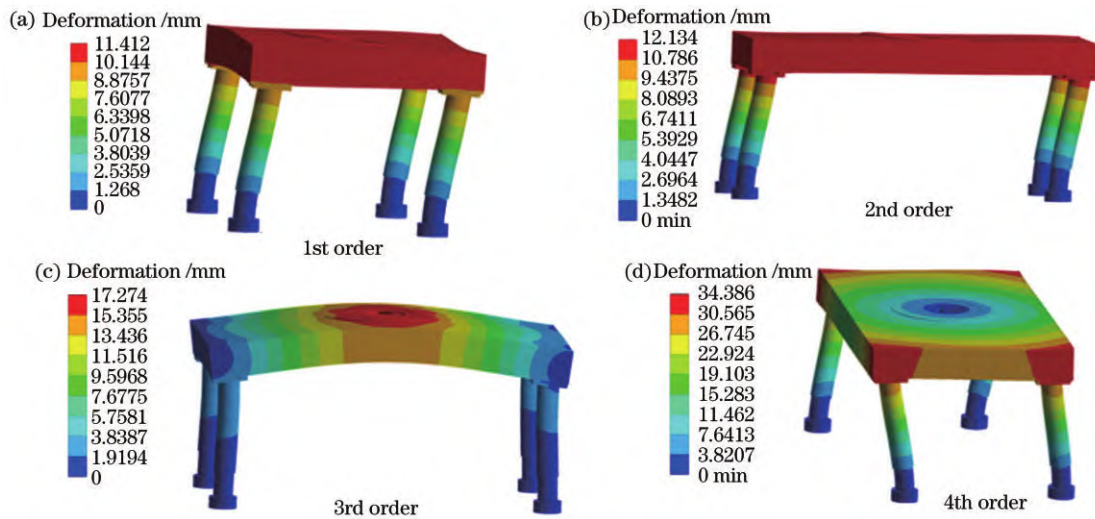


图 8 平台系统前四阶工作模态振型图

Fig. 8 First four order vibration mode shapes of the platform system

表 2 平台系统前四阶工作模态频率

Table 2 First four order vibration mode frequency of the platform system

Order	Frequency/Hz
1st	19.2
2nd	20.8
3rd	42.8
4th	52.1

#### 5 稳定性实验与讨论

根据设计结果,采用方钢管焊接方法制作了支撑平台内部的桁架结构,外围 6 面焊接不锈钢板。平台尺寸为 3150 mm×1830 mm×300 mm,质量为 2000 kg。

支撑平台稳定性实验方案如图 9 所示,包括支撑平台、安装于平台正上方的光电经纬仪、高角平行光管

目标、加速度计、信号采集箱及安装于平台中心的倾角传感器。该经纬仪指向精度为 10", 质量约 3000 kg。支撑平台由四电动伸缩支腿支撑。调平控制系统采用伺服电机与 CAN 通信技术, 具有“一键式”自动调平功能。

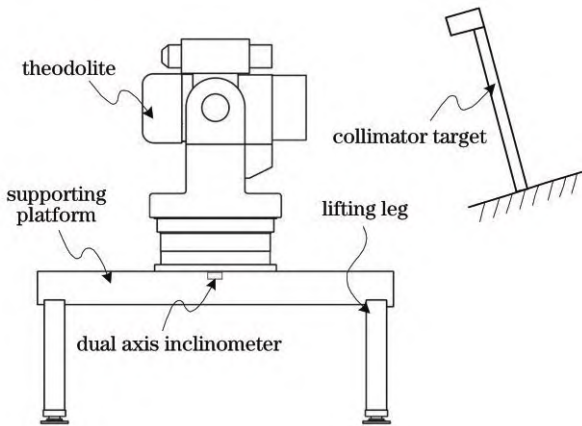


图 9 稳定性实验装置示意图

Fig. 9 Schematic of stability experimental device

光学探测器视场范围内, 光电经纬仪以高角平行光管为目标进行正弦扰动, 控制伺服系统改变加速度大小和摆幅宽度, 施加不同的激励大小, 如表 3 所示, 从而获得平台及经纬仪的关键位置的加速度响应, 该加速度响应能够反映不同工况下平台系统的动态稳定性。

表 3 不同测试条件下的激励大小

Table 3 Incentives on different conditions

Incentive	No. 1	No. 2	No. 3	No. 4	No. 5
Swing / (°)	0.5	1	1	2	4
Angle acceleration / [(°)/s <sup>2</sup> ]	0.5	1	5	10	20

采用 YMC9232 测试信号采集箱, 分别在平台尾部(通道 13)、平台右前侧(通道 12)、经纬仪基座(通道 9、10、11)、转台(通道 6、7、8)、立柱(通道 4、5)和四通(通道 1、2、3)等 7 处安装加速度传感器, 其灵敏度为 100~1000 mV/(m·s<sup>-2</sup>), 采集不同位置处的加速度信息, 现场布置如图 10 所示。

图 11 为方位和俯仰摆幅 1°、角加速度为 1 (°)/s<sup>2</sup> 时, 经纬仪基座位置时域和频域响应加速度波形图。图 12 为方位和俯仰摆幅 4°、角加速度为 20 (°)/s<sup>2</sup> 时, 基座位置时域和频域的响应加速度波形图。可以看出: 角加速度为 1 (°)/s<sup>2</sup> 时, 基座底板位置响应在 0.008~0.033 m/s<sup>2</sup> 范围内变化, 从伺服系统传递到基座的能量极小, 经纬仪动态变化对平台的影响基本可以忽略; 20 (°)/s<sup>2</sup> 时, 经纬仪基座位置产生了最大响应, 幅值为 0.55 m/s<sup>2</sup>; 从频域图可以看出, 当频率为 21.7 Hz 时, 幅值最大为 0.22 m/s<sup>2</sup>, 无明显影响跟踪的共振响应发生。该实验说明车载支撑平台稳定性较

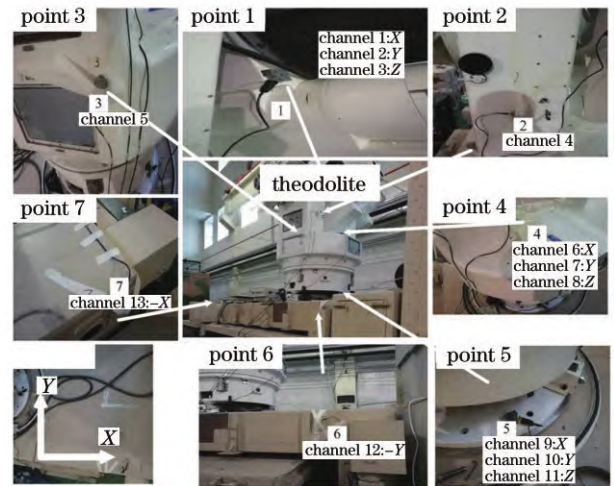


图 10 实验现场布置图

Fig. 10 Experiment layout diagram

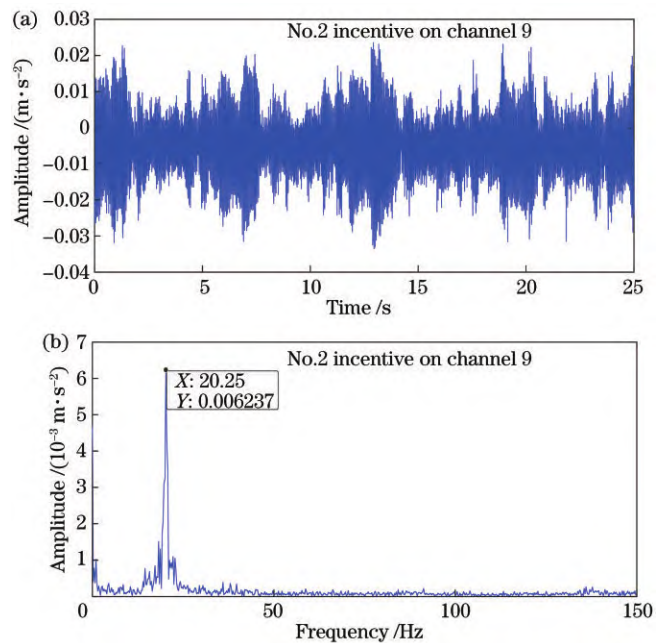


图 11 激励 2 时基座(通道 9)实测响应波形

Fig. 11 Response waveform of No. 2 incentive on channel 9

好, 能够满足光电经纬仪的稳定跟踪要求。

采用双轴倾角传感器测量了经纬仪运动状态的平台晃动量。该传感器测量范围为 ±5° 内, 测量精度为 0.001°。不同角速度和角加速度下的平台晃动幅值如图 13 所示。随着角速度和角加速度的增加, 平台晃动量逐渐增大, 这与测得的经纬仪不同位置处的响应加速度变化趋势一致。当角加速度为 20 (°)/s<sup>2</sup> 时, 平台晃动幅值最大为 7.2"。由于平台支腿的刚度影响, 实验结果稍大于仿真分析结果。

最后, 开展了经纬仪指向精度实验。利用计算机实时记录经纬仪方位角、俯仰角、时间, 同时记录视频图像, 判读目标方位角度脱靶量和俯仰角度脱靶量, 指向精度为方位 13.8"、俯仰 14.9"。该平台已应用于某

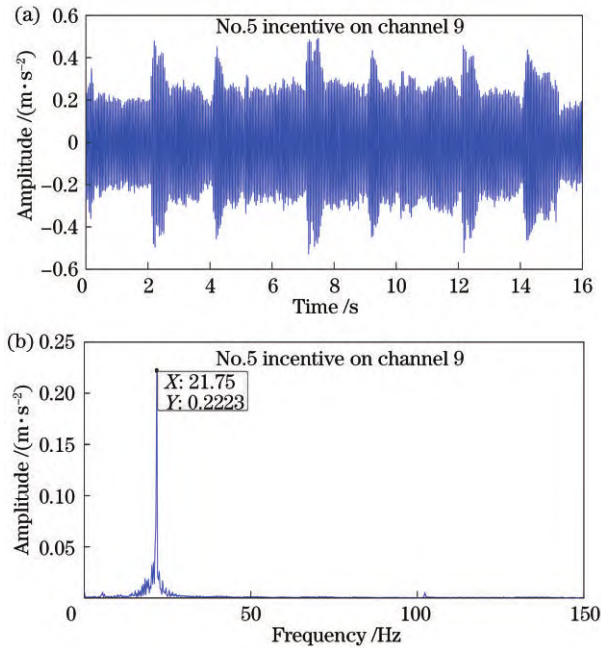


图 12 激励 5 时底座(通道 9)实测响应波形

Fig. 12 Response waveform of No. 5 incentive on channel 9

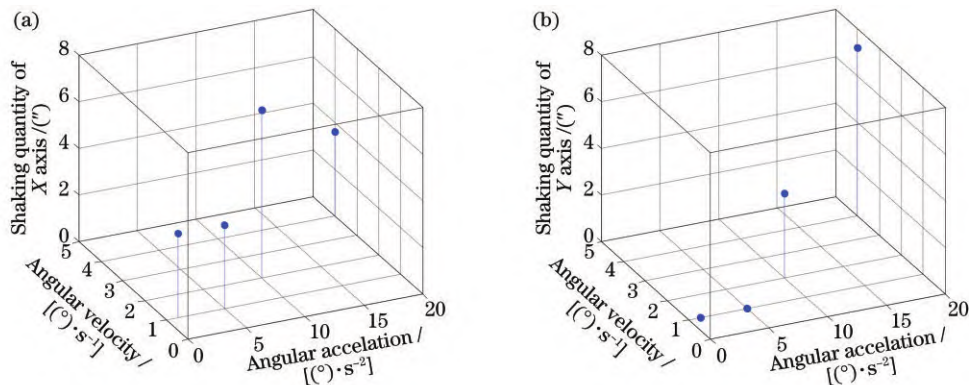


图 13 平台晃动量变化曲线

Fig. 13 Variation curves of the platform shaking

参 考 文 献

[1] 余毅, 刘震宇, 孙志远, 等. 靶场光电测量设备发展现状及展望[J]. 光学学报, 2023, 43(6): 0600002.  
 Yu Y, Liu Z Y, Sun Z Y, et al. Development status and prospect of photoelectric measurement equipment in range[J]. Acta Optica Sinica, 2023, 43(6): 0600002.

[2] 王从敬, 王东, 黄鑫, 等. 大口径 SiC 轻量化主镜的优化与有限元分析[J]. 光学学报, 2021, 41(11): 1122002.  
 Wang C J, Wang D, Huang X, et al. Optimization and finite element analysis of large-aperture SiC lightweight primary mirror [J]. Acta Optica Sinica, 2021, 41(11): 1122002.

[3] Liu R Q, Zhang H, Wang X M, et al. Dynamic modeling and vibration characteristics analysis of a large-scale photoelectric theodolite tracking frame[J]. Machines, 2022, 10(12): 1150.

[4] Xie M L, Ma C W, Liu K, et al. The application of active polarization imaging technology of the vehicle theodolite[J]. Optics Communications, 2019, 433: 74-80.

[5] 姜伟伟, 高云国, 冯栋彦, 等. 大型光电设备基准平面自动调平系统[J]. 光学精密工程, 2009, 17(5): 1039-1045.

型车载光电经纬仪不落地测量系统, 国内靶场测量的实时指向精度优于 15"。

6 结 论

车载支撑平台的稳定性是影响车载光电经纬仪实现高精度不落地测量的关键因素。采用离散体桁架拓扑优化方法设计了一种具有桁架蒙皮式结构的车载支撑平台, 在保证刚度前提下, 支撑平台质量相对减少了 26.5%, 有效提高了平台的比刚度。通过在平台系统不同位置布置加速度传感器, 获得了经纬仪全动态范围跟踪状态下经纬仪基座位置的响应加速度信息, 变化范围为 0.008~0.55 m/s<sup>2</sup>, 峰值出现在 20~21 Hz, 无明显影响经纬仪跟踪性能的共振响应发生。随着经纬仪角速度和角加速度的增加, 支撑平台晃动量逐渐增大, 最大晃动量为 7.2", 平台具有较高的稳定性。该支撑平台已应用于某型车载光电经纬仪不落地测量系统, 实时指向精度优于 15"。所提离散体桁架拓扑优化方法能够快速给出支撑平台的原始构型, 缩短设计周期, 同样适用于其他钢架式承载平台的稳定性设计。

Jiang W W, Gao Y G, Feng D Y, et al. Automatic-leveling system for base-plane of large-size photoelectric equipment[J]. Optics and Precision Engineering, 2009, 17(5): 1039-1045.

[6] 王涛, 唐杰, 宋立维. 车载光电经纬仪的测量误差修正[J]. 红外与激光工程, 2012, 41(5): 1335-1338.  
 Wang T, Tang J, Song L W. Correction of the measuring error of vehicular photoelectric theodolite[J]. Infrared and Laser Engineering, 2012, 41(5): 1335-1338.

[7] 佟刚, 王芳. 车载平台变形对测角误差的影响分析与修正[J]. 光学精密工程, 2011, 19(4): 775-782.  
 Tong G, Wang F. Analysis and correction for influence of vehicle platform deformation on measuring errors[J]. Optics and Precision Engineering, 2011, 19(4): 775-782.

[8] 李增, 吴志勇, 佟刚, 等. 车载经纬仪的静态指向误差补偿[J]. 光学精密工程, 2010, 18(4): 921-927.  
 Li Z, Wu Z Y, Tong G, et al. Pointing error correction for vehicular platform theodolite[J]. Optics and Precision Engineering, 2010, 18(4): 921-927.

[9] 张小虎, 刘进博, 刘铁军, 等. 不稳定平台晃动测量与修正方法研究[J]. 中国科学: 技术科学, 2015, 45(5): 471-475.  
 Zhang X H, Liu J B, Liu T J, et al. Measuring and correcting

- method for shaking platform of vehicle-mounted theodolite[J]. *Scientia Sinica (Technologica)*, 2015, 45(5): 471-475.
- [10] Wang X M, Xie J, Deng J, et al. Topology optimization for improving vibration characteristics of theodolite supporting platform[C]//25th International Congress on Sound and Vibration 2018 (ICSV 25), July 8-12, 2018, Hiroshima, Japan. [S.l.: s.n.], 2018.
- [11] Krog L A, Olhoff N. Optimum topology and reinforcement design of disk and plate structures with multiple stiffness and eigenfrequency objectives[J]. *Computers & Structures*, 1999, 72(4/5): 535-563.
- [12] Shu L, Wang M Y, Fang Z D, et al. Level set based structural topology optimization for minimizing frequency response[J]. *Journal of Sound and Vibration*, 2011, 330(24): 5820-5834.

## Stability of Supporting Platform for Vehicle-Mounted Optoelectronic Theodolite

Gao Qingjia, Wang Chong, Wang Qianglong, Wang Xiaoming, Yu Yi, Liu Zhenyu,  
Liu Yanjun\*

*Changchun Institute of Optics, Fine Mechanics and Physics, Chinese Academy of Sciences, Changchun 130033, Jilin, China*

### Abstract

**Objective** Traditional vehicle-mounted supporting platforms have large shaking amounts and are difficult to meet the requirements of high and non-landing measurement accuracy of the vehicle-mounted optoelectronic theodolite. We design a novel supporting platform with the truss skinned structure based on a discrete topology optimization method with considering the demand for high stability, light weight, and easy manufacturing. The vehicle-mounted theodolite characterized by stronger mobility, faster, and more convenient deployment processes, has been the major trend in test ranges. The supporting platform provides a new measurement reference for vehicle-mounted theodolite. Therefore, the stability of the supporting platform is an important factor enabling theodolite to achieve high-accuracy measurement. Due to the limited size, weight conditions, and dynamic characteristics of theodolite, the platform stability is consistently low. Generally, the shaking amount is over  $40''$ , even up to hundreds of arc seconds. Some appropriate correction methods can be employed to improve the pointing accuracy of the theodolite, but the timeliness is limited. As a result, it is necessary to design a kind of supporting platform featuring high stiffness, good dynamic characteristics, and light weight.

**Methods** A truss discrete topology optimization method is adopted to design the supporting platform. The platform frame is established according to its basic shape, and the design domain and non-design domain of the structure are also determined according to the finite element grids. The solid isotropic material with penalization (SIMP) interpolation model is adopted in the topology optimization. The minimum flexibility is set as an objective function and the volume fraction as a constraint. The topology optimization layout is then obtained (Fig. 3). Based on the above topology optimization results, a detailed model of the optimized platform system, which consists of theodolite, platform, and lifting legs, is developed for simulation (Fig. 5). The platform truss structure is discretized by the truss element. The theodolite has a mass of 30000 N, and the maximum angular accelerations of  $20 (^{\circ})/s^2$ , which are set as the static load and dynamic load in the analysis respectively. The static and modal properties of the supporting platform are simulated successfully, and the supporting platform is also manufactured. The stability experiment is then carried out.

**Results and Discussions** Simulations are conducted to determine the stability of the optimized platform. The mass of the optimized platform is reduced by 411.1 kg to ensure the support stiffness and dynamic characteristics (Table 1). The deformations of the optimized platform under gravity loading are obtained (Fig. 6). The maximum deformation is 0.142 mm, which occurs on the position fixed by the theodolite. The surface tilt of the position is  $3.9''$ . The static deformations under the torques in the direction of the length, width, and height of the platform are also acquired (Fig. 7). The maximum amount of platform shaking is  $4.3''$ , with the sound performance of the platform to resist torque load. The first four vibration mode shapes for the platform system are obtained (Fig. 8). The first order frequency is 19.2 Hz. Square steel tubes are welded to the trusses. The upper and lower platform surfaces are fitted with metal skins for protection and as mounting bases for theodolite and legs. The platform weighs 2000 kg, with the length of 3150 mm, width of 1830 mm, and height of 300 mm. We also set up the experimental apparatus, which consists of the theodolite, the platform, four lifting legs, a dual-axis collimator, and a collimator target (Fig. 9). The theodolite works on the platform and each lifting leg is mounted separately on all four corners of the platform. The legs utilize servo motors and

CAN communication technology to achieve automatic leveling with the help of a program-controlled computer. The theodolite does sinusoidal motion at the set angular accelerations from  $0.5 (^{\circ})/s^2$  to  $20 (^{\circ})/s^2$ . The response accelerations for the basis of theodolite are  $0.008\text{--}0.55 \text{ m/s}^2$  (Figs. 11 and 12). The maximum amplitude is  $0.22 \text{ m/s}^2$  when the frequency is 21.7 Hz. There is no obvious resonance response that affects the tracking performance of the theodolite. The shaking amplitude of the platform is measured by an inclination sensor, with a maximum amount of  $7.2''$ . The pointing error of vehicle-mounted optoelectronic theodolite is also measured, with an accuracy of  $13.8''$  at azimuth and  $14.9''$  at pitch. The supporting platform has a high support stability.

**Conclusions** The stability of the vehicle-mounted supporting platform is an important factor enabling theodolite to achieve high measurement accuracy. In our paper, a novel supporting platform with the truss skinned structure is designed based on the discrete topology optimization method. The mass of the optimized platform is reduced by up to 26.5% to ensure the support stiffness and dynamic characteristics. The stability experiment of the supporting platform is carried out. The response accelerations for the basis of theodolite are  $0.008\text{--}0.55 \text{ m/s}^2$  in the whole angle acceleration range from  $0.5 (^{\circ})/s^2$  to  $20 (^{\circ})/s^2$ . The peak response acceleration appears from 20 Hz to 21 Hz. There is no obvious resonance response that affects the tracking performance of the theodolite. The shaking amplitude of the platform is measured by an inclination sensor. The maximum amount of platform shaking is  $7.2''$ . The supporting platform has a high support stability and has been applied to a vehicle-mounted photoelectric theodolite. The real-time and non-landing pointing accuracy is better than  $15''$ . It is suitable for vehicle-mounted optoelectronic theodolite to achieve high and non-landing measurement accuracy.

**Key words** vehicle-mounted optoelectronic theodolite; non-landing measuring; supporting platform; stability